IEEE Open Journal of
Power Electronics

Received 24 February 2020; revised 24 March 2020; accepted 31 March 2020. Date of publication 20 April 2020;
date of current version 30 April 2020. The review of this article was arranged by Associate Editor Lijun Hang.

Digital Object Identifier 10.1109/OJPEL.2020.2985700

Optimal Design of Integrated Heat Pipe Air-Cooled System Using TLBO Algorithm for SiC MOSFET Converters

MARYAM ALIZADEH [1] (Member, IEEE), ROMINA RODRIGUEZ [1] (Member, IEEE), JENNIFER BAUMAN [2] (Member, IEEE), AND ALI EMADI [1] (Fellow, IEEE)

[1] McMaster Automotive Resource Centre (MARC), McMaster University, Hamilton, ON L8P 0A6, Canada
[2] Electrical and Computer Engineering, McMaster University, Hamilton, ON L8S 4K1, Canada

CORRESPONDING AUTHOR: MARYAM ALIZADEH (e-mail: alizadem@mcmaster.ca)

This work was supported in part by the Canada Excellence Research Chairs (CERC) Program and in part by the Natural Sciences and Engineering Research Council of Canada (NSERC).

ABSTRACT Optimal thermal management system design is critical for power electronic converters to ensure the reliability of power semiconductor switches. Medium power density inverter systems are often air-cooled to ensure an efficient and cost-effective thermal management solution. In addition, using heat pipes as the heat transfer medium between the heat sources and the heat sink can provide lower volume for the entire inverter. This paper investigates the effectiveness of Teaching Learning Based Optimization (TLBO) for finding the optimal forced-air heat sink with heat pipe cooling system to achieve higher fan efficiency and lower inverter packaging volume. The optimal design is found utilizing commercially available fans and heat pipes. The TLBO design optimization is also compared to the highly implemented Particle Swarm Optimization (PSO) and it is found that TLBO uses 20 times fewer iterations than PSO to converge, and that the TLBO results are more robust for different design constraints.

INDEX TERMS Heat pipe, heat sink, inverters, junction temperature, power loss, Particle Swarm Optimization (PSO), SiC MOSFET, Teaching Learning Based Optimization (TLBO), thermal management.

I. INTRODUCTION

Advances in the field of power electronics have resulted in an increase in power density and miniaturization on the device level [1]. One of the critical components used in the design of power converters is power semiconductor switches. Although, silicon (Si) power switches such as IGBTs have been widely used in the power electronics industry for the last few decades, silicon-based technology has some limitations in terms of increasing power density. One of the critical limitations of Si power switches is their relatively low junction temperature operation capability, which often prevents the cooling system design from achieving high power density. However, the introduction of silicon carbide (SiC) power switches has resulted in higher operating temperature limits due to the higher melting temperature of SiC compared to Si. Also, due to the ~3x higher thermal conductivity of SiC compared to Si, heat generated within the semiconductor can be dissipated with a lower temperature drop across the device [2], [3]. Therefore, as there is a trend towards smaller die areas to enable higher switching frequencies, managing the heat dissipation from the component requires more efficient cooling techniques to achieve the thermal requirements of these high-power density components.

The designed power converter in this research is for smart home applications, which utilizes PV as the renewable energy source. The converter is designed for 3 kW power at a nominal input voltage of 48 V, and it consists of a dual active bridge (DAB) converter and an inverter (Fig. 1). The DAB includes the low voltage and high voltage side. The power generated from the PV cells is an input to the high voltage side, and it can either be stored in a battery on the low voltage side or be used for single phase load applications such as home appliances. The switches that are used for the inverter side are TO-247 SiC power MOSFETs from CREE [4].

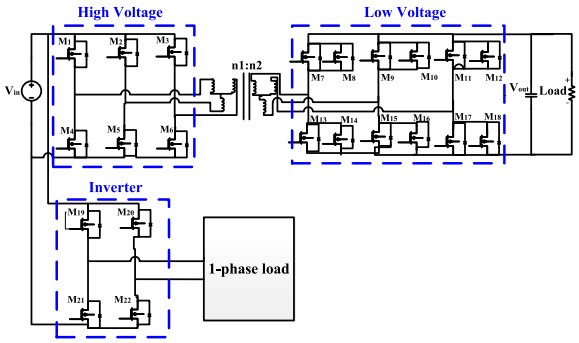

FIGURE 1. Schematic of a 3 kW inverter with DAB power converter.

It is desirable to design power converter systems with minimized packaging to increase power density and reduce weight, which in turn results in more difficult thermal management design. Failure due to thermal fatigue in power electronic systems accounts for 55% of all failures [5], which reiterates the importance of effective heat dissipation. Typical power electronic thermal management systems are over-designed with large heat sinks and the inverter design is not optimized, meaning un-utilized space exists in the system. Therefore, designing a cooling system that can fit the available design space is of high interest. Heat pipes, which have a high thermal conductivity, allow for design of compact thermal management solutions and several modeling and design methods for heat pipe heat exchanger systems have been presented [6], [7]. Thus, optimization of a thermal management solution that utilizes heat pipes with the appropriate optimization algorithm is of high interest in power electronics.

Forced air cooling is an efficient and commonly used technique applied to inverter design, as it has advantages compared to other types of cooling such as: lower complexity than liquid-cooled systems, lower volume, and relatively higher efficiency compared to natural cooling. In addition to preventing the electric components from overheating, the optimal design of a power electronics cooling system should also minimize the weight, volume, and cost and/or maximize the efficiency. The authors in [8] designed a forced air cooling system for minimized weight. Optimizing the cooling system thermal conductivity for different heat sink materials has been done in [9]. The authors in [10] studied and compared the efficiency of forced and natural cooling systems for high power density converters. However, selecting a compatible fan with a heat sink design is a challenge in designing an optimum cooling system. Different fans have different operating points when combined with a specific heat sink. Finding the optimum point according to the inverter's requirements is a challenge that needs to be addressed using an efficient optimization algorithm. Reference [11] performed an optimization for a heat sink in a forced air cooling system for an inverter using MATLAB's genetic algorithm and finite element analysis. In their study, achieving the optimal design point takes more than 130 hours, which requires high computation time and thus delays design progress.

Genetic algorithm or other evolutionary algorithms are widely used in power electronics to find the optimal design for cooling systems [8]–[10], [12], [13]. [8] investigated the system energy efficiency due to different fan selections compared to natural cooling for various heat sink designs. However, all these previous works use optimization algorithms that are dependent on algorithm-controlling parameters, which reduce robustness in the results and cause low convergence rates. Hence, a more robust and fast optimization mechanism is desired. Teaching Learning Based Optimization (TLBO) is a proven robust method that doesn't require algorithm-controlling parameters and can be applied for mechanical design problems [14], [15].

This paper introduces a new approach of using teaching-learning-based optimization (TLBO) for optimizing the thermal design of an air-cooled SiC MOSFET inverter using integrated heat pipes, where heat pipes are used to transfer the heat out of the compact space to a feasible space for heat dissipation in power electronic packages. The contributions of this paper are: (i) introducing an experimentally-validated thermal network model for integrated heat pipe air-cooled heat sink systems with SiC MOSFETS, (ii) proposing an optimization methodology for the design of forced-air cooling systems using commercially available heat pipes and fans to both minimize volume and maximize efficiency, and (iii) using the TLBO algorithm for a power electronic thermal system optimization, which has not been done in prior work. The advantage is that the TLBO algorithm is not dependent on algorithm-controlling parameters, making it more robust than many common heuristic optimization algorithms.

This article is organized as follows. Section II presents the developed thermal model of the heat pipe-heat sink system for the inverter that is used in the optimization. Both a numerical verification with ANSYS and experimental validation of the developed model are detailed. The optimization approach and objective functions are described in Section III. Implementation of the more robust TLBO algorithm and the evolutionary algorithm, PSO, are presented. The resulting optimized cooling solution from the TLBO and PSO algorithm are compared in Section IV. A simulation of the optimal cooling solution is provided to verify the results. Section V summarizes the research presented.

II. COOLING SYTEM DESIGN APPROACH

Heat pipes are a common passive cooling device. In applications with limited space, heat pipes are the most used method for transferring the heat from the device to a location with a larger area for heat dissipation. Heat pipes can be embedded in conductive plates or heat sinks for increasing heat spread or transfer capabilities [1]. Integration of heat pipes in electronic devices has been investigated for automotive applications [16]–[18] due to their high thermal conductivity, efficiency, flexibility, and suitable range of working temperature without consuming any additional electric energy.

A heat pipe is a sealed hollow metal pipe that contains a small amount of liquid to increase heat transfer [19]. Heat

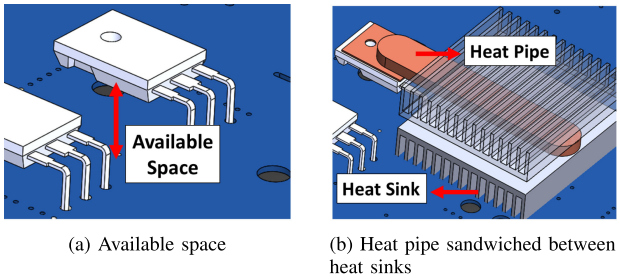

(a) Available space

(b) Heat pipe sandwiched between heat sinks

(c) Side view of the cooling system

(d) Extended proposed cooling system

FIGURE 2. Heat pipe transferring the heat from heat source (case of the MOSFET) to the heat sink.

is conducted from one end of the heat pipe to the opposite end through evaporation of the liquid. Therefore, a heat pipe requires both a heat source and a heat sink. In this particular case the source is the heat dissipated from the switches, and the heat sink is the forced air cooling system.

Forced air cooling is the combination of fans and heat sinks. The fans are implemented for lowering the thermal resistance between the ambient air and the heat sink. This method is the most commonly used cooling system in power converters due to ease of implementation [20]. Forced air cooling system models have been developed and implemented in [8], [9], [12], [13], [21]. The heat sink model was further extended in this research by modeling the heat pipe which is embedded in the air-cooled heat sink.

In this research, like in many practical applications, the cooling system needed to be designed according to the predetermined MOSFET and PCB layout while achieving high power density and low volume. Fig. 2(a) shows the MOSFET layout on the PCB and the available space that is left between the case of the discrete MOSFET and the PCB for mounting the heat sink. To achieve high power density, this space can be used by a possible air-forced cooling system (Fig. 2(b–c)) for the inverter. The system consists of a heat pipe that connects the heat source (case of the MOSFET) to the heat sink and a fan forces the air through the channels of the heat sink. Therefore, the heat sink utilizes the available space which would not be possible without the implementation of heat pipes. Finally, a thin copper plate with the same footprint as the MOSFET is soldered to the heat pipe to secure the MOSFET using a screw and a nut. This design can be extended for a different number of switches in the converter as shown in Fig. 2(d).

In general, the use of heat pipes in a forced-air cooling system allows more flexibility in the physical layout of the PCB and components, specifically reducing the volume of the bulky heat sink. Also, this can simplify PCB layout when

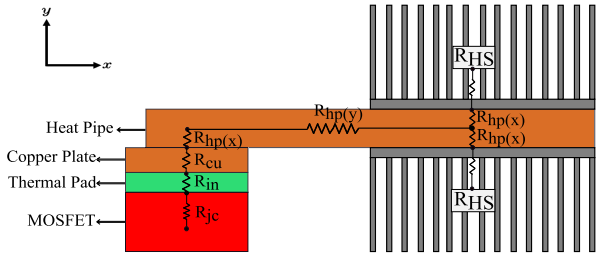

FIGURE 3. Thermal network schematic form junction of heat source to the ambient.

volume is a tight restriction. Thus, though there may be a small additional cost to using heat pipes, the layout/volume advantages can be large depending on the application. This is especially true for demanding applications such as the inverter discussed in the paper, where there is a low height requirement to meet consumer acceptability targets.

A. THERMAL NETWORK FOR MULTIPLE HEAT SOURCES

In order to build an optimized cooling system, the utilization of optimization algorithms is required for the initial design based on different variables that change according to the system's constraints. Optimization of the system through the use of numerical methods such as ANSYS is computationally expensive, thus, a reduced order model such as a thermal network model can be utilized. This optimization implements a thermal network model which is first compared to the numerical results from ANSYS for verification before proceeding forward with the optimization study.

The schematic of the thermal resistance network for Fig. 2(c) from the MOSFET's junction to the ambient is shown in Fig. 3. Total thermal resistance from junction to the ambient can be calculated using (1), where R_{jc} is the thermal resistance of the MOSFET from junction to case, R_{in} is the thermal resistance due to the interfacing thermal pad, R_{cu} is the thermal resistance of the copper plate, $R_{hp(x)}$ and $R_{hp(y)}$ are the thermal resistances of the heat pipe in x and y direction, respectively. R_{HS} is the total thermal resistance of the heat sink attached to the heat pipe. Considering all the aforementioned resistances, the total resistance from junction to ambient, R_{tot}, is

$$R_{tot} = R_{jc} + R_{in} + R_{cu} + R_{hp(x)} + R_{hp(y)} + \frac{1}{2}\left(R_{hp(x)} + R_{HS}\right) \tag{1}$$

If the total thermal resistance is solved for the entire cooling system, then the junction temperature can be solved for as

$$T_j = R_{tot} Q + T_{in} \tag{2}$$

where T_j is the junction temperature, Q is the total heat loss of the device, and T_{in} is the inlet air temperature.

To model the thermal resistance of the heat sink, a single channel of the flat plate fins can be considered as shown in Fig. 4. Since the geometry of the fins and channels are all the same in the entire heat sink, the results for one single fin

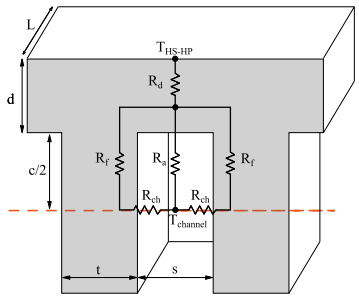

FIGURE 4. Thermal network for the convective and conductive heat transfer through a single channel of a parallel plate fin heat sink.

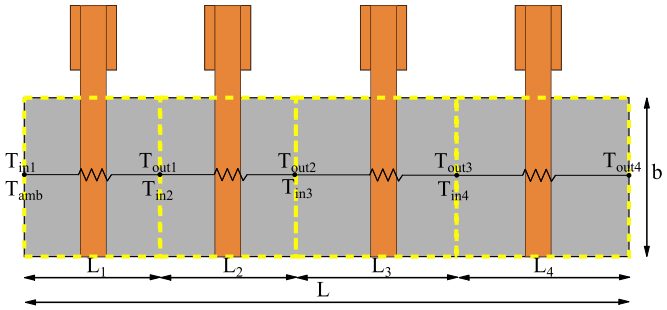

FIGURE 5. Top view of thermal network for multiple heat sources attached to an air-forced cooling system.

can be extended over the entire heat sink composed of any number of fins, n [9]. The thermal network is depicted for heat exchange between the air and the fin surfaces. Following the networks shown in Fig. 4, the total thermal resistance from the surface of the heat sink to ambient air of the fan inlet can be obtained from

$$R_{HS} = R_{cond,f} + R_{conv,f} + R_{\Delta T} \tag{3}$$

The term $R_{cond,f}$ is the result of conductive heat flow through the fins and $R_{conv,f}$ is due to convective heat transfer from the fin surfaces to the air and is defined by

$$R_{cond,f} + R_{conv,f} = \frac{1}{n}\left[R_d + \left(\frac{1}{R_a} + \frac{1}{\frac{1}{2}\left(R_f + R_{ch}\right)}\right)^{-1}\right] \tag{4}$$

R_a and R_{ch} are the thermal resistance caused from convective heat transfer from the base plate exposed to air flow and from the fin surface, respectively. R_f and R_d are the thermal resistances caused from conduction through the fin and base plate thickness, respectively, that can be calculated as

$$R_a = \frac{1}{hLs} \tag{5}$$

$$R_{ch} = \frac{1}{hLc} \tag{6}$$

$$R_f = \frac{c}{tL\lambda_{hs}} \tag{7}$$

$$R_d = \frac{d}{(s+t)L\lambda_{hs}} \tag{8}$$

The convective heat transfer coefficient is calculated by

$$h = \frac{Nu_{m,T}\lambda_{air}}{d_h} \tag{9}$$

where the hydraulic diameter, d_h is calculated as

$$d_h = \frac{2sc}{s+c} \tag{10}$$

and λ_{air} is the thermal conductivity of the air. The mean Nusselt number, $Nu_{m,T}$, for flow in a duct can be applied to the fin channels and is defined as [22]

$$Nu_{m,T} = 7.55 + \frac{0.024(x^*)^{-1.14}}{1 + 0.0358(x^*)^{-0.64}Pr^{0.17}} \tag{11}$$

where the distance, x^*, in the direction of the air-flow is defined as

$$x^* = \frac{L}{d_h RePr} \tag{12}$$

The Reynolds number, Re, for the channels is defined as

$$Re = \frac{2V}{n(s+c)\nu_{air}} \tag{13}$$

and ν_{air} is the kinematic viscosity of air. The velocity of the air flowing through the channels, V, is solved for by setting the pressure drop of the fan equal to the pressure drop of the heat sink

$$kdP_{fan}(V) = dP_{HS}(V) \tag{14}$$

where k is the fin spacing ratio of the heat sink defined as

$$k = \frac{s}{b/n} \tag{15}$$

The geometric variables d, c, t, s and L are all depicted in Fig. 4, and b is the width of the heat sink as it is shown in Fig. 5.

As the air moves from inlet to outlet through the heat sink, its temperature will increase and the term $R_{\Delta T}$ is considered to account for the temperature rise

$$R_{\Delta T} = \frac{0.5}{\rho_{air}C_{p,air}\upsilon} \tag{16}$$

where ρ_{air} and $C_{p,air}$ are the density and specific heat of the air, respectively, and υ is the volumetric air flow.

For the case with multiple heat sources on the heat sink, the thermal model can have additional nodes (Fig. 5) and each node can be studied as an individual heat sink system where the inlet temperature of node i is equal to the outlet temperature of the previous node, $i-1$ such that

$$\begin{cases} T_{in}(i) = T_{out}(i-1) & i = [2, \ldots, N_{hs}] \\ T_{in}(1) = T_{amb} \end{cases}$$

where N_{hs} is the number of heat sources. Thus, the MOSFET's junction temperature of each node can be calculated from

$$T_j(i) = R_{tot}(i)Q(i) + T_{in}(i) \tag{17}$$

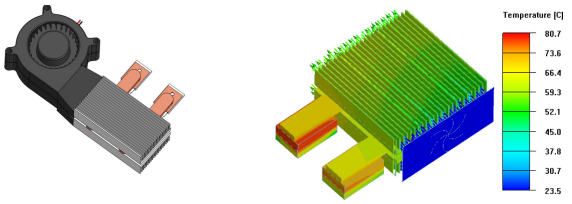

(a) 3D model of the setup (b) ANSYS model of the setup

FIGURE 6. ANSYS model of cooling design at a power loss of 43 W.

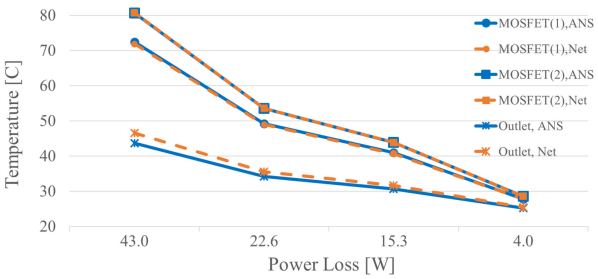

FIGURE 7. Comparison of ANSYS (ANS) and proposed thermal network (Net) results for the temperature of: inlet air, outlet air, and the two MOSFETs at different power losses.

B. THERMAL NETWORK MODEL VERIFICATION

In order to examine the performance of the proposed reduced-order thermal model, a design is modeled in ANSYS Icepak and the results are compared to the proposed analytical model. Fig. 6(a) shows a simple heat pipe heat sink design that uses a commercially available fan to force air through the heat sink. The heat pipe that is used in this model is a conventional heat pipe from QATS [23] and the thermal resistance is measured experimentally. The experimental characterization of the off-the-shelf planar heat pipes was performed by imposing a heat source and heat sink on the heat pipes and measuring the temperature distribution along the axial direction [24].

The MOSFETs and proposed thermal solution are simulated for different power losses. An example of the ANSYS Icepak solution is shown in Fig. 6(b). The predicted temperature of the MOSFET's case, inlet and outlet air flow (from the heat sink) by the numerical model are compared with the proposed thermal network model results.

Fig. 7 compares the predicted temperature of inlet air, outlet and the two MOSFETs from the proposed model to the ANSYS results at different power ratings. The reduced thermal model agrees with the ANSYS model within 1%.

C. THERMAL NETWORK MODEL EXPERIMENTAL VALIDATION

An experimental test is also performed to validate the thermal network model. Two heat pipes are sandwiched between two copper heat sinks and a fan is attached through a duct to simulate the cooling setup (Fig. 8). To simulate the losses from the MOSFETs, 1 ohm resistors with the same footprint as the TO-247 were used as the heat sources and the maximum expected power loss of 43 W was imposed with the power supply.

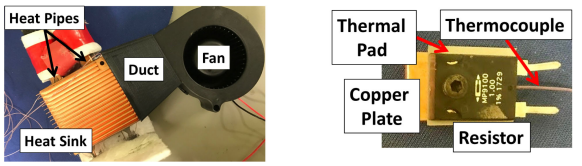

(a) Proposed cooling system setup (b) Close-up of experimental test

FIGURE 8. Experimental setup to validate proposed thermal model.

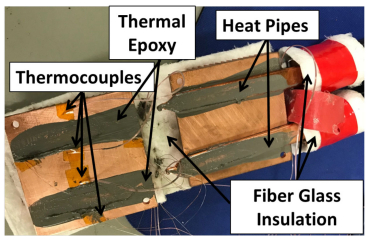

FIGURE 9. Thermocouples are mounted on the heat sink and the setup is insulated using fiber glass fabric.

TABLE I Error From Thermal Model Compared to Temperature Measurements From Experimental Tests and ANSYS Results for Different Power Losses

Power Loss [W]	Measurement point	Temperature [°C]			Error [%]	
		Thermal network	Exp.	ANSYS	Exp.	ANSYS
43	Resistor 1	71.9	78.1	72.5	8.6	0.8
	Resistor 2	80.8	87.8	80.7	8.7	0.1
	Outlet Air	46.5	41.9	43.7	9.9	6.0
23	Resistor 1	49.0	53.4	49.3	9.0	0.6
	Resistor 2	53.6	58.0	53.6	8.2	0.0
	Outlet Air	35.6	32.4	34.2	9.0	3.9
15	Resistor 1	40.7	44.0	41.0	8.1	0.7
	Resistor 2	43.9	46.7	43.9	6.4	0.0
	Outlet Air	31.7	29.5	30.7	6.9	3.2
4	Resistor 1	27.8	29.7	27.8	6.8	0.0
	Resistor 2	28.6	30.0	28.6	4.9	0.0
	Outlet Air	25.5	24.1	25.3	5.5	0.8

Several T-type thermocouples are mounted on different locations of the heat sink and on the case of the resistors, as well as the inlet and outlet of the heat sink's channels to measure the air temperature. A data acquisition device, Omega USB TC-08, is used for recording the temperature and a power supply is connected to the power dissipating devices to simulate the heat losses for various power ratings. Fiber glass fabric is used to insulate the resistors, heat pipes, and the heat sink to ensure that heat loss is completely dissipated through the heat sink channels (Fig. 9).

The tests are carried out for a power loss of 43, 23, 15 and 4 W in order to compare the experimental data to the analytical results. As shown in Table 1, the measured temperatures from the experiments are within 10% with an average error of 7%, and the results from ANSYS model are within 6% with an average error of 1% of the predicted results from the proposed thermal network.

III. OPTIMIZATION OF COOLING DESIGN

The optimization of a cooling system design can minimize the weight, volume, or cost, or maximize the power density for the desired working conditions. The goal of this research is to design a cooling system with the minimum volume for

TABLE II Characteristics of Investigated Fans for Cooling System

Fan #	Manufacturing no.	Input power [W]	Max air flow [CFM]	Max static pressure [inch H2O]
1	BM-7530B-134	3.6	13.6	0.60
2	BM-7530B-224	1.9	9.6	0.27
3	B5020	1.4	6.0	0.20
4	CBM-5015V-140	0.78	3.5	0.40
5	CBM-6015V-150	1.25	5.7	0.44

the inverter and achieve maximum power efficiency of the cooling system. In this study the geometrical configurations of the heat sink along with the fan selection options are optimized. Two objective functions, volume of the converter and power efficiency of the cooling system, have been selected as the design space. Since the fan is the only component that consumes power, the efficiency, η, of the cooling system is defined by the power efficiency of the fan by

$$\eta = \frac{dP_T v}{P_{in}} \tag{18}$$

dP_T is the pressure drop for the corresponding volumetric air flow, v, of the fan's operating point and P_{in} is the power consumption of the fan.

The length and width of the cooling system are determined within the power converter package which can be maximum of 155 and 50 mm, respectively, and the only parameter that changes the volume of the entire converter is the height of the heat sink, h_f. Hence, by finding the minimum height it can be assured that the volume is minimized. In addition, the maximum junction temperature that the SiC MOSFETs can operate for this inverter is 150 °C. The optimization problem has been limited to six degrees of freedom represented by number of fins, n, fin height c, fin thickness t, heat sink width b, base plate thickness d and fan selection. In this study, five different fans (properties in Table 2) with various air flow, static pressure and power consumption range are selected to integrate with the heat sink model and study the optimal design.

Fig. 10 shows the optimization procedure for designing the cooling system. The discrete design variables in this optimization problem are fan selection and the number of fins, n. Thus, the proposed method finds the optimal design in two steps: 1) applying the optimization algorithm in a loop for number of fins within its limits and 2) repeating the first step for each fan option. The optimization process starts by selecting one fan and the lower boundary of the number of fins. An initial design for the population of N_{tot} is generated for different heat sink geometry variables: t, d, b, c and n. Then, each design's fitness is evaluated, new population members are created by using an optimization algorithm and the best design is found. This process continues until reaching the maximum number of iterations. Afterwards, since the minimum volume of the converter is of higher interest in this study than the fan power efficiency, the minimum height (local optimal design) of the heat sink based on the optimization constraints and variables is found for different numbers of fins. The design that resulted in the lowest height for the corresponding number of fins is

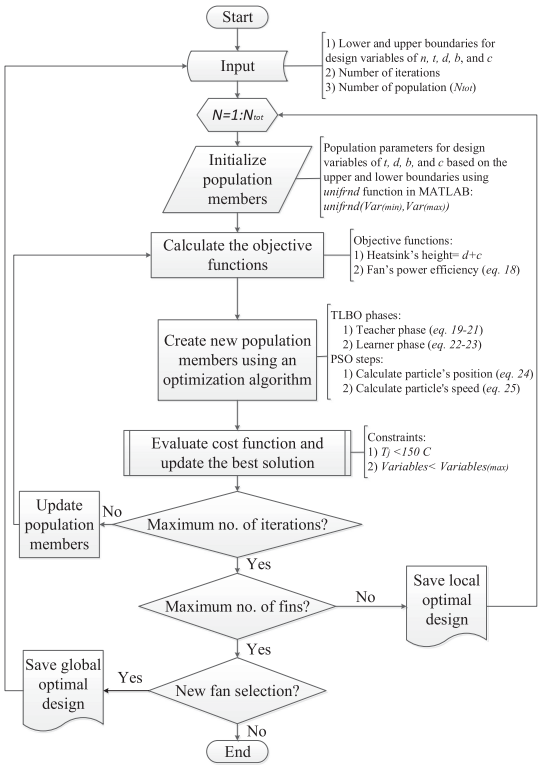

FIGURE 10. The process of the cooling system design optimization.

saved as the best for each fin number (local optimal design). Eventually, the corresponding fan power efficiency values for each achieved minimum height are compared to investigate the best optimal design (global optimal design) which minimizes height and maximizes cooling system efficiency. This process is repeated for all five fans and at the end, the global and local optimum designs for all the fans are studied and compared to find the most desirable design point.

An optimization process finds the maximum or minimum of a function relative to a set of parameters, which represents a range of choices available that satisfies a set of constraints. The evolutionary optimization algorithms require common controlling parameters like population size, number of generations, etc. In addition to common controlling parameters, each algorithm has its own algorithm-specific control parameters. The most commonly used evolutionary optimization methods are the Genetic Algorithm (GA) and Particle Swarm Optimization. Nonetheless, GA determines almost the optimal solution for a complex problem that includes a large number of variables and constraints. Determining the optimum controlling parameters including crossover and mutation rates cause some difficulties for this method, since changing the controlling parameters can affect the algorithm performance drastically. Similarly, in the case of using the PSO algorithm, controlling parameters such as inertia weight, and social and cognitive coefficients have a large impact on the algorithm effectiveness [14].

Therefore, an optimization technique which requires less algorithm controlling parameters is of more interest for the

optimum design of the cooling system in this research. Teaching–Learning-Based Optimization (TLBO) is a robust and proven optimization method for seeking global solutions for continuous non-linear functions, which also has low computations and high consistency [14]. The implementation of TLBO requires only determining the common controlling parameters such as population size and number of generations, so there is no need for any of the algorithm-specific controlling parameters, which leads to robust results [25]. To investigate the robustness of the Teaching Learning Based Optimization (TLBO) algorithm, the results are compared to the widely used Particle Swarm Optimization (PSO) algorithm.

A. TEACHING LEARNING BASED OPTIMIZATION (TLBO)

The TLBO method is based on the influence of a teacher on the output of learners in a class, where the output can be considered as the grades. The teacher is considered as the most knowledgeable person in the class who shares his or her knowledge with the learners. Thus, the quality of a teacher influences the grades of the learners. TLBO is a population-based optimization algorithm that utilizes a population of solutions that proceed to the most desired solution. In contrast with other population-based optimization techniques, there are no algorithm controlling-parameters involved in TLBO, which makes the implementation simpler. The process of TLBO is divided into two sections: Teacher Phase, where the learners learn from the teacher and the Learner Phase, where the learners learn and improve their level of knowledge through interaction with other learners in the class.

1) TEACHER PHASE

Students' knowledge can be improved through the inputs from their teacher. Hence, the class can be defined with the level of the teacher's knowledge (T_i), the mean of learner's grades (G_i), and the level of each learner's knowledge (X_i). Every teacher (T_i) tries to improve the level of the entire class (G_i) close to its own level (G_{new}). Therefore, the solution can be updated according to the difference between the existing and new mean of the class. Since the teacher might be able to change the mean for a better level or not, a teaching factor (T_F) is assigned that can be either 1 or 2, and r_i is a number between [0,1] that randomly decides what the mean value is. Hence, the new level of each student ($X_{new,i}$) can be improved according to the mean difference using (19–21) [26], and if the new level of a student gives better function value, it is accepted for proceeding the optimization.

$$\Delta_G = r_i(G_{new} - T_F G_i) \tag{19}$$

$$T_F = round[1 + rand(0, 1)] \tag{20}$$

$$X_{new,i} = X_{old,i} + \Delta_G \tag{21}$$

2) LEARNER PHASE

Students' knowledge can also be improved through interaction with other students. One grade (X_i) will improve if the student learns something from another student who has a higher level of knowledge. Hence for a class with a population of N_{pop}, the learners' level of knowledge will modify by comparing each student (X_i) within the population of $i = [1 : N_{pop}]$ to another random student (X_j). If X_i is a better student than X_j, the level of knowledge will change to (22), otherwise it will be (23). At the end of the comparison loop for the entire student population (N_{pop}), if X_{new} results in a better objective value ($f(X_{new})$), X_{new} is accepted as the best optimization point [26].

$$X_{(new,i)} = X_{(old,i)} + r_i(X_i - X_j) \tag{22}$$

$$X_{(new,i)} = X_{(old,i)} + r_i(X_j - X_i) \tag{23}$$

B. PARTICLE SWARM OPTIMIZATION (PSO)

Particle swarm optimization (PSO) is an evolutionary algorithm that simulates the movement of flocks or birds searching for food. In PSO, the objective function determines the fitness of each individual's solution. Each solution is described as a particle in the search space. The particles fly through the search space to find the minimized or maximized value returned by the objective function. Typically, the particles are located randomly in the search space and they evaluate their fitness at their position. Afterwards, each particle moves to a new location that can upgrade its fitness over the previous position. The movement is based on the particle's own experience and other particles in the group (swarm). Hence, the PSO algorithm consists of a swarm that includes m particles, and each particle's position represents a possible solution according to the fitness function. Each particle moves toward a new location according to three factors: its own inertia, its own most optimal position, the entire swarm's most optimal solution [27]. The position (x) and speed (v) of each particle is defined by

$$x_i^{k+1} = x_i^k + v_i^{k+1} \tag{24}$$

$$v_i^{k+1} = w.v_i^k + c_1.r_1^k(pbest_i^k - x_i^k) + c_2.r_2^k(gbest_i^k - x_i^k) \tag{25}$$

$pbest_i^k$ and $gbest_i^k$ represent personal and global best positions of the i^{th} particle at its k^{th} iteration, w is the inertial weight, c_1 is the personal learning coefficient and causes the particle to move toward its personal best, c_2 is the global learning coefficient that leads the particle toward the best position the swarm has been experienced. r_1^k and r_2^k are random numbers in the range of [0, 1] [27]. Inertia weight, personal and global learning coefficients, and maximum value of velocity are the PSO controlling parameters that need to be tuned in the algorithm in order to proceed to the optimum solutions.

The optimization is run for 5 different fans using the TLBO and PSO algorithms. For all configurations, the number of iterations and populations is 200 and 20, respectively. The PSO controlling parameters are defined based on the studies that have been done on stability and convergence in multi-dimensional complex spaces for PSO problems in [28] and shown in Table 3.

TABLE III PSO Algorithm Controlling Parameters

Inertia Weight	0.72984
Personal Learning Coefficient (c_1)	1.49618
Global Learning Coefficient (c_2)	1.49618
Maximum Velocity	$0.02(Variables_{max} - Variables_{min})$

TABLE IV Optimal Design Points for Each Fan Obtained From PSO and TLBO Algorithms Considering 40 W Power Loss on Each MOSFET

Fan #	Efficiency [%]	Height [mm]	Max T_j [°C]	n	t [mm]	c [mm]	b [mm]
1	5.4	9.6	150	12	0.5	7.6	49.9
2	3.3	13.7	150	12	0.5	11.7	49.9
3	1.04	22	155	11	0.5	20.0	50.0
4	2.0	20.5	189	15	0.5	18.5	50.0
5	2.5	18.7	150	13	0.5	16.7	49.9

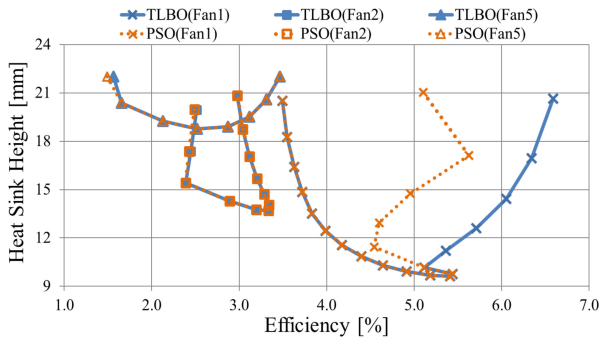

FIGURE 11. The heat sink height versus efficiency for feasible optimal designs from the optimization utilizing TLBO and PSO for different fans.

IV. OPTIMIZATION RESULTS AND VERIFICATION

Applying the TLBO and PSO algorithms resulted in similar global optimum points for each fan (presented in Table 4), while each algorithm achieves different local optimum points as portrayed in Fig. 11. The results from Table 4 show that fan number 3 and 4 do not satisfy the limitation of maximum junction temperature of 150° C. However, fan number 1, 2, and 5 are feasible designs within the junction temperature requirement.

A. PERFORMANCE COMPARISON

In order to study the performance of the TLBO algorithm, the height, h_f, and power efficiency, η, of the cooling system designs that met the design requirements are compared in Fig. 11. Each point in Fig. 11 is the local optimum design for the corresponding number of fins, n. The y-axis represents the heat sink height and x-axis is the power efficiency of the fan. As the height decreases and fan power efficiency increases, the design is more desirable. As it can be observed, utilizing fan number 1 is the most desirable design with a power efficiency of 5.4% and heat sink height of 9.6 mm.

Comparing the results from TLBO to PSO shows that fan number 2 and 5 both produce almost the same local optimum points for each algorithm. The results for fan number 1 in Fig. 11 demonstrate the inability of PSO to find the local optimum designs at certain number of fins. Even though the global best points that are achieved for each fan by both algorithms are the same (Table 4), it is important to use a robust algorithm that can find the best local optimum points as well, since number of fins with limited volume constraint can be crucial for manufacturing requirements.

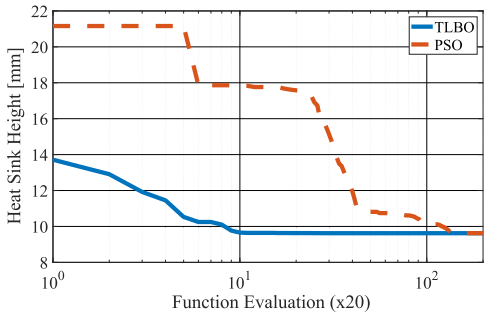

FIGURE 12. Convergence plots for finding the minimum height as the optimal heat sink design using TLBO and PSO algorithms applied to fan number 1.

Furthermore, the objective function value's convergence during the entire optimization for all the iterations can be studied. Fig. 12 compares the convergence rate of TLBO (blue solid line) to PSO (red dashed line) for finding the minimum heat sink height using fan number one. It's depicted that TLBO is converging around 200 iterations and PSO is converging at 4000 iterations. Therefore, it is observed that TLBO has better performance than PSO in the entire optimization process in terms of producing better results and a faster convergence rate which means lower number of evaluations for finding the optimum design and low computational time of about 90 seconds.

In addition, the use of the proposed TLBO optimization process can reduce component costs because a minimum volume will lead to minimum packaging costs. It can also reduce operating costs because the higher fan efficiency will translate into lower energy consumption by the cooling system. Moreover, since TLBO uses 20 times fewer iterations compared to the widely-used evolutionary algorithm PSO, it will result in computation and design time savings, which can lower development costs.

B. ANSYS VERIFICATION

The optimization results show that the configuration with fan number 1 achieves the highest efficiency and lowest height compared to the other design points. Therefore, this most optimal point is selected for verifying the design performance. A model with the same design parameters as this point and inverter's operation condition is simulated in ANSYS Icepack (Fig. 13). The simulation is run for the MOSFET power loss of 40 watts using fan number 1, and the temperature of the MOSFETs lead frames are observed.

Table 5 compares the results obtained from the proposed thermal model to the ANSYS simulation. The slight difference in the values is because each MOSFET in the thermal model is considered as one control volume. Hence, the entire

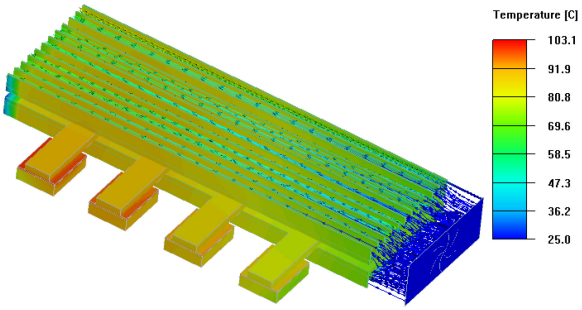

FIGURE 13. Temperature contours for the optimal point at 40 watts power loss in ANSYS Icepack.

TABLE V MOSFET's Case Temperature at Optimal Point Obtained From Thermal Model and ANSYS at 40 W Power Loss

	1^{st} MOSFET	2^{nd} MOSFET	3^{rd} MOSFET	4^{th} MOSFET
ANSYS [°C]	89.1	93.9	97.9	103.1
Thermal Model [°C]	86.5	89.3	94.1	102.0
Error [%]	2.9	4.9	3.9	1.1

cooling system is divided into 4 segments, and the temperature of each MOSFET is evaluated as a single point in the area of the corresponding node. However, in ANSYS the system is simulated and solved with larger number of nodes, so the results are different within 5% error.

The further-most MOSFET from the fan gets warmer compared to the other MOSFETs (Table 5), and the error for the warmest MOSFET which is critical for temperature constraints is about 1%. Hence it can be concluded that the proposed thermal model is highly accurate and adequate for finding the optimal design.

V. CONCLUSION

An integrated forced-air heat pipe embedded heat sink cooling system is designed for an inverter application.

The biggest advantages of the proposed cooling system over previous research is integrating passive and active cooling methods in order to design a very compact, power efficient cooling system by using: heat pipes, plate-fin heat sinks and fans, through the implementation of a very robust optimization algorithm. In addition, integrating fans with heat sinks drops the efficiency of the fan performance due to the change in cross-sectional area for the air flow. Therefore, an optimization scheme needed to be applied to find the optimum design point which minimizes power consumption of the fan. A reduced-order thermal model for the proposed cooling system is developed. The thermal model is expanded for multiple heat sources application and is used in the optimization scheme.

A simulation is modeled in ANSYS Icepack and the accuracy of the developed thermal model compare to the numerical simulation was about 99%. In addition, a setup was built and tested with multiple heat sources to validate the developed thermal model experimentally. The average error between the thermal model and the experimental results is ∼7% tested at various power losses.

The validated thermal model was applied in Teaching Learning Based Optimization (TLBO) and Particle Swarm Optimization (PSO) algorithms to find the optimum cooling system design. It is concluded that the results found by TLBO are more robust compared to PSO in terms of finding the optimum design and achieving faster convergence rate.

Furthermore, two of the most crucial issues in power converters packaging, volume and power efficiency, were discussed during the optimization process for six different design parameters. These parameters included of number of fins, fin height, fin thickness, heat sink width, base plate thickness and fan selection options, while considering critical operating temperature, packaging size and manufacturability constraints. Although the proposed optimization method was applied to an inverter with SiC MOSFETS with TO-247 packaging, the same optimization approach can be used for different discrete MOSFET packages or for IGBT modules which require an air-cooled thermal management design. The thermal resistance value in the switch thermal model would have to be updated for the new switch package based on its datasheet.

Finally, the most optimum design that is found from the optimization process is simulated in ANSYS and verified with the optimization results.

ACKNOWLEDGMENT

This work is dedicated to the memory of Iman Aghabali and Mehdi Eshaghian.

REFERENCES

[1] E. Laloya, Ó. Lucía, H. Sarnago, and J. M. Burdío, "Heat management in power converters: From state-of-the-art to future ultrahigh efficiency systems," *IEEE Trans. Power Electron.*, vol. 31, no. 11, pp. 7896–7908, Nov. 2016.

[2] J. Wang, A. Huang, W. Sung, Y. Liu, and B. Baliga, "Smart grid technologies," *IEEE Ind. Electron. Mag.*, vol. 3, no. 2, pp. 16–23, Jun. 2009.

[3] S. Anandan and V. Ramalingam, "Thermal management of electronics: A review of literature," *Thermal Sci.*, vol. 12, no. 2, pp. 5–26, Jan. 2008.

[4] CREE, "C2m0025120d, SiC power MOSFET C2M MOSFET technology N-channel enhancement mode," 2015. [Online]. Available: https://www.mouser.ca/datasheet/2/90/c2m0025120d-838591.pdf

[5] H. Wang, M. Liserre, and F. Blaabjerg, "Toward reliable power electronics: Challenges, design tools, and opportunities," *IEEE Ind. Electron. Mag.*, vol. 7, no. 2, pp. 17–26, Jun. 2013.

[6] G. Righetti, C. Zilio, S. Mancin, and G. A. Longo, "Heat pipe finned heat exchanger for heat Recovery: Experimental results and modeling," *Heat Transfer Eng.*, vol. 39, no. 12, pp. 1011–1023, Jul. 2018.

[7] W. Srimuang and P. Amatachaya, "A review of the applications of heat pipe heat exchangers for heat recovery," *Renewable Sustain. Energy Rev.*, vol. 16, no. 6, pp. 4303–4315, Aug. 2012.

[8] C. Gammeter, F. Krismer, and J. W. Kolar, "Weight optimization of a cooling system composed of fan and extruded-fin heat sink," *IEEE Trans. Ind. Appl.*, vol. 51, no. 1, pp. 509–520, Jan. 2015.

[9] U. Drofenik, G. Laimer, J. W. Kolar, O. Strategy, and H. Power, "Theoretical converter power density limits for forced convection cooling," in *Proc. Int. PCIM Europe Conf.*, Nuremberg, Germany, Jun. 2005, pp. 608–619.

[10] D. Christen, M. Stojadinovic, and J. Biela, "Energy efficient heat sink design: Natural versus forced convection cooling," *IEEE Trans. Power Electron.*, vol. 32, no. 11, pp. 8693–8704, Nov. 2017.

[11] T. Wu, Z. Wang, B. Ozpineci, M. Chinthavali, and S. Campbell, "Automated heatsink optimization for air-cooled power semiconductor modules," *IEEE Trans. Power Electron.*, vol. 34, no. 6, pp. 5027–5031, Nov. 2018.

[12] U. Drofenik, G. Laimer, and J. Kolar, "Pump characteristic based optimization of a direct water cooling system for a 10-kW/500-kHz Vienna rectifier," *IEEE Trans. Power Electron.*, vol. 20, no. 3, pp. 704–714, May 2005.
[13] B. Wrzecionko, D. Bortis, and J. W. Kolar, "A 120°C ambient temperature forced air-cooled normally-off SiC JFET automotive inverter system," *IEEE Trans. Power Electron.*, vol. 29, no. 5, pp. 2345–2358, May 2014.
[14] R. Rao, V. Savsani, and D. Vakharia, "Teaching–learning-based optimization: A novel method for constrained mechanical design optimization problems," *Comput.-Aided Des.*, vol. 43, no. 3, pp. 303–315, Mar. 2011.
[15] R. Rao and K. More, "Optimal design of the heat pipe using TLBO (teaching–learning-based optimization) algorithm," *Energy*, vol. 80, pp. 535–544, Feb. 2015.
[16] D. Deng, J.-P. Cheng, S.-C. Zhang, and F.-G. Ge, "Theoretical and experimental validation study on automotive air-conditioning based on heat pipe and LNG cold energy for LNG-fueled heavy vehicles," *Heat Mass Transfer*, vol. 53, no. 8, pp. 2551–2558, Aug. 2017.
[17] J. Murua, P. Estevez, I. Alonso, A. Arrizabalaga, I. Ibarbia, and T. Nieva, "Application of heat pipe based refrigeration system for an electric train traction converter. an experimental study case," in *Proc. 13th Eur. Conf. Power Electron. Appl.*, Barcelona, Spain, Sep. 2009, pp. 1–11.
[18] A. Driss, S. Maalej, and M. C. Zaghdoudi, "Electro-thermal modeling of power igbt modules by heat pipe systems," in *Proc. Int. Conf. Eng. MIS*, Monastir, Tunisia, May 2017, pp. 1–7.
[19] X. Chen, H. Ye, X. Fan, T. Ren, and G. Zhang, "A review of small heat pipes for electronics," *Appl. Thermal Eng.*, vol. 96, pp. 1–17, Mar. 2016.
[20] A. Blinov, D. Vinnikov, and T. Lehtla, "Cooling methods for high-power electronic systems," *Scientific J. Riga Tech. Univ. Power Elect. Eng.*, vol. 29, no. 1, pp. 79–86, Jan. 2011.
[21] U. Drofenik and J. W. Kolar, "Thermal power density barriers of converter systems," in *Proc. 5th Int. Conf. Integr. Power Syst.*, Nuremberg, Germany, vol. 1, Mar. 2008, pp. 1–5.
[22] S. Kakac, R. Shah, and W. Aung, *Handbook of Single-Phase Convective Heat Transfer*. Hoboken, NY, USA: Wiley, 1987.
[23] Advanced Thermal Solutions, "Performance round and flat heat pipes," U.S, p. 17, 2012. [Online]. Available: https://www.qats.com/Products/Heat-Pipes
[24] M. Alizadeh, "Thermal management of a dual active bridge converter for smart home applications: Design of an optimal integrated forced air heat-pipe embedded heat sink cooling system," Master's thesis, Dept. Mech. Eng., McMaster Univ., Hamilton, ON, Canada, Feb. 2019
[25] R. V. Rao and V. Patel, "Multi-objective optimization of heat exchangers using a modified teaching-learning-based optimization algorithm," *Appl. Math. Modelling*, vol. 37, no. 3, pp. 1147–1162, Feb. 2013.
[26] S. K. Panigrahi and S. Pattnaik, "Empirical study on clustering based on modified teaching learning based optimization," in *Proc. 2nd Int. Conf. Intell. Comput., Commun. Convergence*, Bhubaneswar, India, Jan. 2016, pp. 442–449.
[27] M. Juneja and S. K. Nagar, "Particle swarm optimization algorithm and its parameters: A review," in *Proc. Int. Conf. Control, Comput., Commun. Mater.*, Allahbad, India, Oct. 2016, pp. 1–5.
[28] M. Clerc and J. Kennedy, "The particle swar—Explosion, stability, and convergence in a multidimensional complex space," *IEEE Trans. Evol. Comput.*, vol. 6, no. 1, pp. 58–73, Aug. 2002.

MARYAM ALIZADEH (Member, IEEE) received the B.Sc. degree in mechanical engineering from Amirkabir University of Technology, Tehran, Iran, in 2016 and the M.A.Sc. degree in mechanical engineering from McMaster University, Hamilton, ON, Canada, in 2019. She was an intern as a software developer for design automation in power electronics applications with Infineon Technologies, Villach, Austria, in 2018. She is currently a member of the Mechanical Design and Thermal Management Group, McMaster Automotive Resource Center (MARC), Hamilton, ON, Canada. Her research interests include machine learning, artificial intelligence application for design automation, thermal management in power electronics, electric machines, as well as vehicle modeling and control.

ROMINA RODRIGUEZ (Member, IEEE) received the B.S. and M.S. degrees in mechanical engineering from the University of California, Berkeley, CA, USA and the Ph.D. degree in mechanical engineering from McMaster University, Hamilton, ON, Canada, in 2019. She was a Mechanical Engineer with the Thermal Design & Analysis Group, Northrop Grumman between 2012 and 2014 in California. Her research interests include thermal management of power electronics and electric machines, as well as investigating energy harvesting technologies.

JENNIFER BAUMAN (Member, IEEE) received the B.Sc. and Ph.D. degrees in electrical engineering from the University of Waterloo, Waterloo, ON, Canada, in 2004 and 2008, respectively. From 2009 to 2016, she was the Director of Research with CrossChasm Technologies, where she led the modeling team on a wide variety of automotive projects. She is currently an Assistant Professor of electrical engineering with McMaster University, Hamilton, ON, Canada. She is a registered Professional Engineer and an Associate Editor for the IEEE OPEN JOURNAL OF POWER ELECTRONICS. Her current research interests include power electronic converters for electrified powertrains (including wide bandgap devices), vehicle design, modeling, and control, and EV interactions with the smart grid.

ALI EMADI (Fellow, IEEE) received the B.S. and M.S. (with highest distinction) degrees in electrical engineering from the Sharif University of Technology, Tehran, Iran, in 1995 and 1997, respectively, and the Ph.D. degree in electrical engineering from Texas A&M University, College Station, TX, USA, in 2000. He is the Canada Excellence Research Chair Laureate with McMaster University, Hamilton, ON, Canada. He is also the holder of the NSERC/FCA Industrial Research Chair in Electrified Powertrains and Tier I Canada Research Chair in Transportation Electrification and Smart Mobility. Before joining McMaster University, he was the Harris Perlstein Endowed Chair Professor of Engineering and the Director of the Electric Power and Power Electronics Center and Grainger Laboratories, Illinois Institute of Technology, Chicago, where he established research and teaching facilities as well as courses in power electronics, motor drives, and vehicular power systems. He was the Founder, Chairman, and President of Hybrid Electric Vehicle Technologies, Inc. (HEVT)—a university spin-off company of Illinois Tech. He has been the recipient of numerous awards and recognitions. He was the Advisor for the Formula Hybrid Teams with Illinois Tech and McMaster University, which won the GM Best Engineered Hybrid System Award in 2010, 2013, and 2015 competitions. He is the principal author or coauthor of more than 450 journal and conference papers as well as several books, including *Vehicular Electric Power Systems* (2003), *Energy Efficient Electric Motors* (2004), *Uninterruptible Power Supplies and Active Filters* (2004), *Modern Electric, Hybrid Electric, and Fuel Cell Vehicles* (2nd ed., 2009), and *Integrated Power Electronic Converters and Digital Control* (2009). He is also the Editor of the Handbook of *Automotive Power Electronics and Motor Drives* (2005) and *Advanced Electric Drive Vehicles* (2014). He is the Co-Editor of the *Switched Reluctance Motor Drives* (2018). He was the Inaugural General Chair of the 2012 IEEE Transportation Electrification Conference and Expo (ITEC) and has chaired several IEEE and SAE conferences in the areas of vehicle power and propulsion. He is the founding Editor-in-Chief for the IEEE TRANSACTIONS ON TRANSPORTATION ELECTRIFICATION.